Squeezing based analytical variational method for the biased quantum Rabi model in the ultrastrong coupling regime

Weijie Xie[1]**, Bin-Bin Mao**[2]**, Guangzhuo Li**[1]**, Weihang Wang**[1]**, Chen Sun**[1]**, Yimin Wang**[3]**, Wen-Long You**[4,5] **and Maoxin Liu**[1,6]

[1] State Key Laboratory of Information Photonics and Optical Communications & School of Science, Beijing University of Posts and Telecommunications, Beijing 100876, People's Republic of China
[2] Department of Physics, Hong Kong University, Hong Kong, People's Republic of China
[3] Communications Engineering College, Army Engineering University, Nanjing 210007, People's Republic of China
[4] College of Science, Nanjing University of Aeronautics and Astronautics, Nanjing 211106, People's Republic of China
[5] School of Physical Science and Technology, Soochow University, Suzhou, Jiangsu 215006, People's Republic of China
[6] Beijing Computational Science Research Center, Beijing 100094, People's Republic of China

E-mail: liumaoxin@bupt.edu.cn

Abstract

In order to obtain the ground state of the biased quantum Rabi model in the ultrastrong coupling regime, a generalized squeezing rotating-wave approximation method including the displacement and the squeezing transformations is proposed in this work. While considering the deformation of the oscillator state, our method evidently improves the generalized variational method. The analyses of a few physical quantities show that our method works well especially in the ultrastrong coupling and large atomic frequency regime.

Keywords: squeezing, biased quantum Rabi model, variational method, ultrastrong coupling

(Some figures may appear in colour only in the online journal)

1. Introduction

The quantum Rabi model (QRM) [1, 2] describes the coupling between a two-level atom and a bosonic field. Such model is of fundamental importance, since it has been widely applied in modern physics, such as in optical waveguides [3], superconducting circuits [4, 5], trapped ion [6] and so on. Given its great importance, there have been numerous theoretical studies on the Rabi model finding approximated solutions [7–9, 10–21]. Despite a great achievement of all those studies, the exact solution of QRM was only obtained recently [22–24]. This analytical solution, however, is in the form of composite transcendental function defined in power series, and it is not feasible to analyze the miscellaneous physical quantities of the QRM. Thus, theoretical research of finding the optimal analytical solution still attracts much attention.

In early days, the atom-field coupling strength of the Rabi model achieved in experiments is much smaller than the frequency of the field. Therefore, the QRM can be further simplified into the renowned Jaynes Cummings model (JCM) through rotating wave approximation (RWA), which ignores the counter-rotating-wave (CRW) terms [25]. With the tremendous development of experimental technologies, the strength of the light-matter coupling greatly increases. Recently one remarkable achievement is the realization of ultrastrong coupling [26–28]. To this end, the RWA breaks down [29, 30] since the effect of CRW terms is no longer negligible. In this respect, the generalized RWA (GRWA) [7] with a fixed displacement is proposed by considering the effect of CRW terms. However, the GRWA method does not perform well enough in the ultrastong coupling regime when the resonator frequency is small, and a more general variational method which relaxes the displacement is proposed [8, 9]. These approximation methods have been applied in the family of the QRM [8, 10–20].

The ultrastrong coupling of the QRM has been experimentally achieved in circuit quantum electrodynamics system due to operational conveniences [26–28, 30], and the so-called bias term is naturally involved. Compared to the standard form of the QRM, the additional bias term may bring in complication but more physics. For instance, the parity symmetry in the QRM is broken due to the presence of this bias. Given the interesting physics that come together with the bias term, it is therefore highly desirable to study the corresponding model analytically. Though there already exists some analytical discussions based on the GRWA and generalized variational method (GVM) for the biased QRM [9, 11], we find that there is still space to improve the accuracy in the ultrastrong coupling regime. The crucial idea to construct a close ground state in the widely used methods (e.g. GRWA, GVM) is to figure out the displacement of the oscillator. Since a quantum harmonic oscillator not only can be displaced but also can be squeezed, it is natural and necessary to consider the squeezing effect of the oscillator. The squeezing effect of the oscillator can be introduced in the same way with the displacement. The squeezing deformation of quantum state in the QRM can be naturally captured by an additional squeezing transformation applied onto the oscillator state, and thus substantial improvements may be anticipated. The squeezing plays an important role in high precision applications. For instance, it can be used to improve the sensitivity of gravity-wave detectors [31]. In quantum optics, the most common and useful way to create entangled states has been through squeezing [32–35], and it has been recognized that the intrinsic nonlinearities of atoms lead to quadrature squeezing [36–40]. With regard to this consideration, a generalized squeezing RWA (GSRWA) [15, 41] with an additional squeezing transformation was proposed to study the anisotropic QRM and shows high accuracy in large parameter regime. In this work, by taking both the displacement and squeezing transformations, we adopt the GSRWA by introducing a squeezing transformation to study the underlying physics of the biased QRM. The variational parameters in the GSRWA are determined by minimizing the

ground-state energy. In order to show the improvement of our methods over the GVM, we also calculate several physical quantities by GVM and numerical method for comparison.

The paper is outlined as follows. In section 2, we give the Hamiltonian of the biased QRM and shows the details of our method. In section 3, we show the results of several physical quantities. In section 4, the applicable regime is discussed and a brief summary is finally given.

2. Model and analytical solution

Conventionally, the Hamiltonian of the biased QRM reads [42–45]

$$H_B = \omega a^\dagger a + g\sigma_x(a + a^\dagger) + \Delta\sigma_z + \epsilon'\sigma_x, \tag{1}$$

where $a^\dagger$ (a) is the creation (annihilation) operator of the bosonic oscillator with frequency ω, Pauli matrix σ_z describes the two-level system with energy splitting 2Δ, $\epsilon'\sigma_x$ is the biased term, and g is the coupling strength between the oscillator and the qubit. Taking a rotation of the spin along y-axis and replacing the parameters with $\epsilon' = \epsilon/2$ and $\Delta = \Omega/2$, we can obtain

$$\begin{aligned}
H &= e^{i\frac{\pi}{4}\sigma_y} H_B e^{-i\frac{\pi}{4}\sigma_y} \\
&= \omega a^\dagger a - \frac{\Omega}{2}\sigma_x + \frac{\epsilon}{2}\sigma_z + g\sigma_z(a^\dagger + a).
\end{aligned} \tag{2}$$

For convenience, the following discussions are focusing on Hamiltonian equation (2) by default.

The model Hamiltonian in equation (2) can be divided into the main part and the perturbation as

$$H = H_{\text{do}} + H_{\text{p}}. \tag{3}$$

Here the displaced oscillator

$$H_{\text{do}} = \omega a^\dagger a + g\sigma_z(a^\dagger + a) \tag{4}$$

is treated as the non-perturbed Hamiltonian, and

$$H_{\text{p}} = -\frac{\Omega}{2}\sigma_x + \frac{\epsilon}{2}\sigma_z \tag{5}$$

can be considered as the perturbation. The ground state of the unperturbed Hamiltonian in equation (4) is doubly degenerate, which can be expressed by the direct production of a spin eigenstate and a corresponding coherent state:

$$|G\rangle_{\text{do}} = |\pm_z\rangle \otimes |\mp\lambda_0\rangle, \tag{6}$$

where $|\pm_z\rangle$ are the eigenstates of σ_z with eigenvalues ± 1, and $|\pm\lambda_0\rangle = e^{\pm\lambda_0(a^\dagger - a)}|0\rangle$ are the coherent states with $\lambda_0 = g/\omega$.

Taking the perturbation H_{p} into accounted, the ground state can be approximated by the linear combinations of equation (6) in the subspace of degenerate states:

$$|G\rangle_{\text{do}} = \frac{1}{\sqrt{2}}\left(|+_z\rangle \otimes |-\lambda\rangle - |-_z\rangle \otimes |\lambda\rangle\right), \tag{7}$$

where λ is unfixed, since H_{p} effectively reduces the distance of the displaced oscillator. The quantitative value of the λ can be determined by a variational manner, namely, minimizing the ground-state energy function of the full Hamiltonian. The state in equation (7) is the starting

point of the GVM, which has proven to perform better than the adiabatic approximation and the GRWA in a number of cases [8, 10, 12].

To proceed, the displacement in equation (7) can be understood through the unitary transformation on the vacuum state $|\tilde{G}\rangle_{\text{do}} = U_{\text{do}} |G\rangle_{\text{do}}$, i.e.

$$|\tilde{G}\rangle_{\text{do}} = [\frac{1}{\sqrt{2}} (|+_z\rangle - |-_z\rangle) \otimes |0\rangle], \tag{8}$$

where $|0\rangle$ is the vacuum Fock state, and the incorporated displacement unitary operator is

$$U_{\text{do}} = e^{-\lambda\sigma_z(a^\dagger - a)}. \tag{9}$$

Correspondingly, the Hamiltonian in the transformed representation can be expressed as

$$H' = U_{\text{do}} H U_{\text{do}}^\dagger. \tag{10}$$

Here λ is introduced as a variational parameter rather than being fixed as $\lambda = g/\omega$ in GRWA, and this difference makes GVM obtain better accuracy. The transformed Hamiltonian reads

$$H' = H_0' + H_1' + H_2' + H_3', \tag{11}$$

where

$$
\begin{aligned}
H_0' &= \omega a^\dagger a + \frac{\epsilon}{2}\sigma_z + (\omega\lambda^2 - 2\lambda g), \\
H_1' &= (g - \omega\lambda)\sigma_z(a^\dagger + a), \\
H_2' &= -\frac{\Omega}{2}\sigma_x \cosh[2\lambda(a^\dagger - a)], \\
H_3' &= -\frac{\Omega}{2} i\sigma_y \sinh[2\lambda(a^\dagger - a)].
\end{aligned}
\tag{12}
$$

The hyperbolic cosine and sine terms can be further expanded as [46]

$$
\begin{aligned}
&\cosh[2\lambda(a^\dagger - a)] \\
&= F_0(a^\dagger a) + \sum_{k=0}^{\infty}[(a^\dagger)^{2k}F_{2k+1}(a^\dagger a) - F_{2k}(a^\dagger a)a^{2k}].
\end{aligned}
\tag{13}
$$

and

$$
\begin{aligned}
&\sinh[2\lambda(a^\dagger - a)] \\
&= \sum_{k=0}^{\infty}[(a^\dagger)^{2k+1}F_{2k+1}(a^\dagger a) + F_{2k+1}(a^\dagger a)a^{2k+1}].
\end{aligned}
\tag{14}
$$

The function F_m is defined as

$$F_m(n) = e^{-2\lambda^2}(2\lambda)^m \frac{n!}{(n+m)!} L_n^m(4\lambda^2), \tag{15}$$

where m and n are integers, and

$$L_n^m(x) = \sum_{i=0}^{n}(-x)^i \frac{(n+m)!}{(m+i)!(n-i)!i!}, \tag{16}$$

is the Laguerre polynomial. The detailed calculations see the appendix.

Similar to the displacement effect, the squeezing effect can be considered by a squeezing unitary operator

$$U_{\rm s} = {\rm e}^{\frac{\beta}{2}\left[a^2 - \left(a^\dagger\right)^2\right]}. \tag{17}$$

One can easily obtain the transformation of creation and annihilation bosonic operators as

$$
\begin{aligned}
U_{\rm s} a U_{\rm s}^\dagger &= a^\dagger\sinh\beta + a\cosh\beta,\\
U_{\rm s} a^\dagger U_{\rm s}^\dagger &= a\sinh\beta + a^\dagger\cosh\beta.
\end{aligned} \tag{18}
$$

Substitute equations (18) into (11) and the transformed Hamiltonian $\widetilde{H} = U_{\rm s} H' U_{\rm s}^\dagger$ is rewritten as

$$\widetilde{H} = \widetilde{H}_0 + \widetilde{H}_1 + \widetilde{H}_2 + \widetilde{H}_3, \tag{19}$$

with

$$
\begin{aligned}
\widetilde{H}_0 &= \frac{\omega}{4}({\rm e}^{2\beta} + {\rm e}^{-2\beta} - 2) + \frac{\omega}{2}({\rm e}^{2\beta} + {\rm e}^{-2\beta})a^\dagger a\\
&\quad + \omega\lambda^2 - 2g\lambda + \frac{\epsilon}{2}\sigma_z,\\
\widetilde{H}_1 &= (g - \omega\lambda)\sigma_z(a^\dagger + a),\\
\widetilde{H}_2 &= -\frac{\Omega}{2}\sigma_x\cosh[2\lambda {\rm e}^{-\beta}(a^\dagger - a)],\\
\widetilde{H}_3 &= -\frac{\Omega}{2}{\rm i}\sigma_y\sinh[2\lambda {\rm e}^{-\beta}(a^\dagger - a)].
\end{aligned} \tag{20}
$$

We note that in the bosonic Fock space $\widetilde{H}_0$ only has the diagonal terms, and $\widetilde{H}_1$ shows the off-diagonal terms with the first order of a ($a^\dagger$). By comparison, $\widetilde{H}_2$ and $\widetilde{H}_3$ are more complicated. More precisely, $\widetilde{H}_2$ can be expanded as the sum of even power of a and $a^\dagger$, while $\widetilde{H}_3$ undertakes the sum of odd power of a and $a^\dagger$. It is noteworthy that the coefficients of diagonal terms in $\widetilde{H}_0$ are evidently amplified through the squeezing transformation comparing with H'_0 in (12), while the off-diagonal contributions in equation (20) are either unchanged or reduced. Especially for the variational parameter $\lambda = g/\omega$ chosen in GRWA, $\widetilde{H}_1$ is vanishing. For the ultra-strong coupling regime we are interested in, we only consider diagonal terms of the Hamiltonian (19) in the following calculations, which leads to an effective adiabatic Hamiltonian:

$$
\begin{aligned}
\widetilde{H}_{\rm eff} &= \frac{\omega}{4}(\gamma + 1/\gamma - 2) + \frac{\omega}{2}(\gamma + 1/\gamma)a^\dagger a\\
&\quad + \omega\lambda^2 - 2g\lambda + \frac{\epsilon}{2}\sigma_z - \frac{\Omega}{2}\sigma_x F'_0(N),
\end{aligned} \tag{21}
$$

where $F'_0(N) = {\rm e}^{-2\lambda^2 {\rm e}^{-2\beta}} L_N^0(4\lambda^2 {\rm e}^{-2\beta})$ and $\gamma = {\rm e}^{-2\beta}$ is defined for convenience. It is obvious that the Hamiltonian in equation (21) is analytically solvable. The basis can be chosen as $|\pm_z, n\rangle$, where $|\pm_z\rangle$ are the eigenstates of σ_z with eigenvalues ± 1, and $|n\rangle$ is the Fock state. The Hilbert space can be divided into different subspaces, in which the effective Hamiltonian equation (21) can be recast into the following form:

$$\widetilde{H}_n(\lambda, \gamma) = \begin{pmatrix} \epsilon_n^- & R_n \\ R_n & \epsilon_n^+ \end{pmatrix}, \tag{22}$$

where $\epsilon_n^{\pm} = \frac{\omega}{4}(\gamma + 1/\gamma - 2) + \omega(\gamma + 1/\gamma)n/2 + \omega\lambda^2 - 2g\lambda \pm \epsilon/2$, and $R_n = -\Omega F_0'(n)/2$. From equation (22), the eigenstates and eigenvalues depending on the displacement variable λ and the squeezing variable γ can be easily obtained as

$$E_n^{\pm}(\lambda, \gamma) = \frac{\epsilon_n^- + \epsilon_n^+ \pm \sqrt{\left(\epsilon_n^- - \epsilon_n^+\right)^2 + 4R_n^2}}{2}, \tag{23}$$

and

$$|\widetilde{\phi}_n^{\pm}(\lambda, \gamma)\rangle = A_n^{\pm}|-z, n\rangle + B_n^{\pm}|+z, n\rangle, \tag{24}$$

where

$$A_n^{\pm} = \pm\sqrt{\frac{1}{2}\left[1 \pm \frac{\epsilon_n^- - \epsilon_n^+}{\sqrt{\left(\epsilon_n^- - \epsilon_n^+\right)^2 + 4R_n^2}}\right]},$$

$$B_n^{\pm} = \sqrt{\frac{1}{2}\left[1 \mp \frac{\epsilon_n^- - \epsilon_n^+}{\left(\epsilon_n^- - \epsilon_n^+\right)^2 + 4R_n^2}\right]}. \tag{25}$$

The ground-state energy reads

$$E_G(\lambda, \gamma) = \frac{\omega}{4}(\gamma + 1/\gamma - 2) + \omega\lambda^2 - 2g\lambda$$
$$- \frac{1}{2}\sqrt{\epsilon^2 + \Omega^2 e^{-4\lambda^2\gamma}}. \tag{26}$$

Taking $\gamma = 1$, the obtained energy spectra in equation (26) recover the GVM results [9]:

$$E_G^{GVM}(\lambda) = \omega\lambda^2 - 2g\lambda - \sqrt{\epsilon^2 + \Omega^2 e^{-4\lambda^2}}/2. \tag{27}$$

If one further set the variational parameter $\lambda = g/\omega$, the GRWA result is recovered as

$$E_G^{GRWA} = -g^2/\omega - \frac{1}{2}\sqrt{\epsilon^2 + \Omega^2 e^{-4(g/\omega)^2}}/2. \tag{28}$$

The variational parameters λ and γ in the GSRWA vary with ω, Ω and ϵ, and they can be determined by minimizing the $E_G(\lambda, \gamma)$ by solving $\frac{\partial E_G}{\partial \lambda} = 0$ and $\frac{\partial E_G}{\partial \gamma} = 0$. These two nonlinear equations can not be easily solved in the analytical way. However, in the ultratrong coupling regime we interested in, the approximate solutions are

$$\lambda \approx \frac{g}{\omega + \Omega^2 e^{-4\lambda_0^2}/\sqrt{\epsilon^2 + \Omega^2 e^{-4\lambda_0^2}}}, \tag{29}$$

and

$$\gamma \approx 1 + \delta, \tag{30}$$

where $\lambda_0 = \frac{g}{\omega + \Omega^2/\sqrt{\Omega^2 + \epsilon^2}}$ and $\delta = \frac{-2\Omega^2\lambda^2}{\omega\sqrt{\epsilon^2 + \Omega^2}}$. With determined values of λ and γ, we finally obtain the analytical formula of the ground-state wavefunction,

$$|\tilde{G}\rangle = |\widetilde{\phi}_0^-(\lambda, \gamma)\rangle = -\sqrt{\frac{1}{2}[1 + \frac{\epsilon}{\sqrt{\epsilon^2 + \Omega^2(F_0'(0))^2}}]}|-z, 0\rangle + \sqrt{\frac{1}{2}[1 - \frac{\epsilon}{\sqrt{\epsilon^2 + \Omega^2(F_0'(0))^2}}]}|+z, 0\rangle, \tag{31}$$

and the physical observables can thus be calculated.

Before going on, we would like to discuss the difference between our analytical method and the GVM. Equations (29) and (30) show that even if the parameter λ takes the same value as that in the GVM, another parameter γ may play an essential role in lowering the ground-state energy. When g and Ω are small enough, the optimized γ in our method approaches to 1, which is the exact value presumed in the GVM. However, when g and Ω increase, the optimal value of γ will no longer be 1. In other words, our method improves the precision of variational method when g and Ω are sizeable.

3. The observables and comparison with other methods

With the analytical ground-state wave function equation (31) in hand, in order to show the accuracy of the GSRWA quantitatively, we calculate several physical observables to compare with the results obtained by the GVM. The numerically exact diagonalized results are also involved as a benchmark. The quantum average of a physical observable Q is $\langle Q \rangle = \langle G|Q|G \rangle$, where $|G\rangle = U_{\mathrm{do}}^{\dagger} U_{\mathrm{s}}^{\dagger} |\tilde{G}\rangle$. In this work, we take the ground-state energy $E_{\mathrm{G}} = \langle H \rangle$, the mean photon number $\langle a^{\dagger} a \rangle$, the spin orientation $\langle \sigma_x \rangle$, and the correlation $\langle \sigma_z (a^{\dagger} + a) \rangle$ for illustration. For convenience, we set $\omega = 1$ as an energy unit.

The ground-state energy obtained is given in equation (26). Figures 1(a) and (b) show the ground-state energy of the biased Rabi model as a function of g for different parameters. We see that both the results obtained by the GSRWA and the GVM agree well with the numerical ones for small coupling strength g. With the increase of g, the deviations between the GVM results and the numerical ones enlarges. In contrast, our results fit quite well with the exact ones. Figures 1(c) and (d) show the ground-state energy of the system as a function of Ω and ϵ. It is obvious that our results are better than the GVM. From these comparisons, we find that the GSRWA works much better for large g and large Ω than the GVM. The precision has been greatly improved in a wide parameter regime.

Next we focus on the mean photon number

$$\langle a^{\dagger} a \rangle = \frac{1}{4}(\gamma + 1/\gamma - 2) + \lambda^2, \tag{32}$$

the spin orientation

$$\langle \sigma_x \rangle = \frac{\Omega \mathrm{e}^{-4\lambda^2 \gamma}}{\sqrt{\epsilon^2 + \Omega^2 \mathrm{e}^{-4\lambda^2 \gamma}}}, \tag{33}$$

and the qubit-cavity correlation

$$\langle \sigma_z (a^{\dagger} + a) \rangle = -2\lambda. \tag{34}$$

As is shown in figure 2, it is obvious that our results is quite close to the numerical results for large g, where there are clear deviations for the GVM results.

Another interesting quantity characterizing the squeezing effect is the square of the squeezing strength

$$\langle (a^{\dagger} - a)^2 \rangle = -\gamma. \tag{35}$$

In figure 3, we make the comparison of $\langle (a^{\dagger} - a)^2 \rangle$ calculated by different methods. One observes the result obtained by GVM is a constant -1, but in our method, γ changes with other parameters. The result of $\langle (a^{\dagger} - a)^2 \rangle$ through our method is in good agreement with the
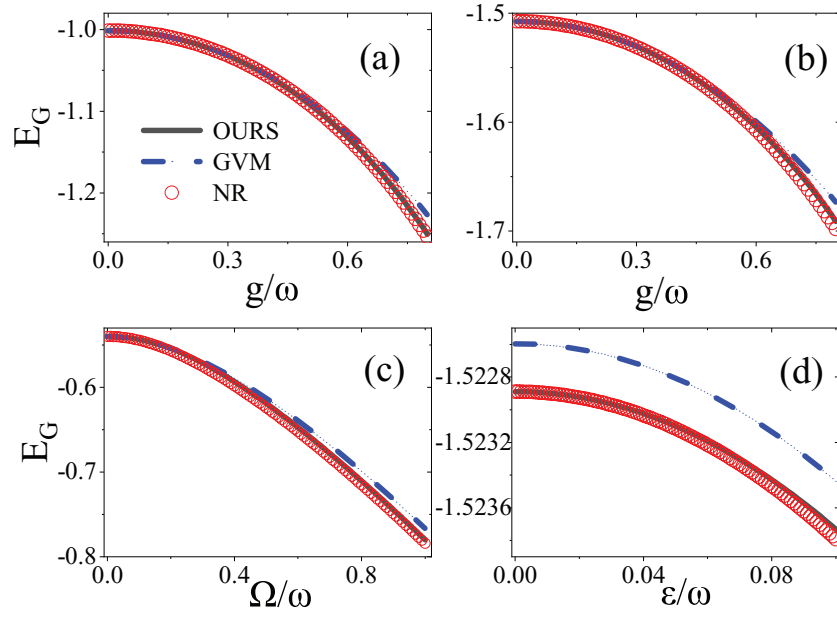
Figure 1. The ground-state energy E_G as a function of g, Ω or ϵ for different parameters. (a) $\Omega = 2$, $\epsilon = 0.1$; (b) $\Omega = 3$, $\epsilon = 0.3$; (c) $g = 0.7$, $\epsilon = 0.1$; (d) $\Omega = 3$, $g = 0.3$.
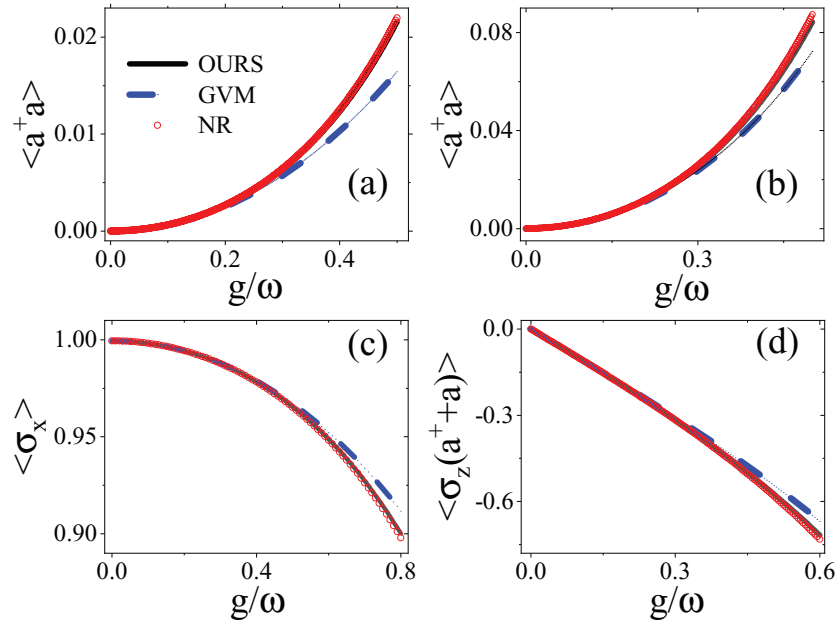

Figure 2. $\langle a^\dagger a \rangle$, $\langle \sigma_x \rangle$ and $\langle \sigma_z(a^\dagger + a) \rangle$ as a function of g/ω for different parameters. (a) $\Omega = 3$, $\epsilon = 0.1$; (b) $\Omega = 1$, $\epsilon = 0.1$; (c) $\Omega = 3$, $\epsilon = 0.1$; (d) $\Omega = 1$, $\epsilon = 0.1$.
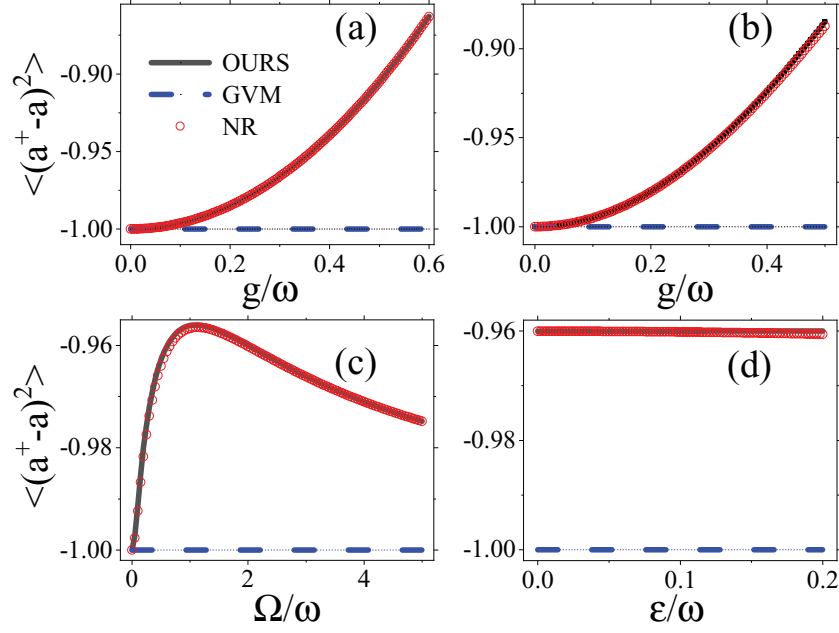
Figure 3. $\langle (a^\dagger - a)^2 \rangle$ as a function of g, Ω and ϵ for different parameters. (a) $\Omega = 3$, $\epsilon = 0.1$; (b) $\Omega = 1$, $\epsilon = 0.1$; (c) $g = 0.7$, $\epsilon = 0.1$; (d) $\Omega = 2$, $g = 0.3$.

numerical results when Ω/ϵ is large, which indicates that it is necessary to take the squeezing effect into account, and our GSRWA method is a convincing way to reveal the squeezing effect of the ground-state wave function.

4. Discussion and conclusion

As an approximation, it is necessary to discuss the applicable range of the method we proposed. It is shown that the GSRWA work quite satisfyingly for large g. According to the so-called polaron picture [47], in such ultrastrong coupling regime, the ground-state energy can be well approximated by a single oscillator. Although some numerical methods have already considered the squeezing effect [48], the analytical results are relatively rare for an intuitive picture The parameter λ describes the displacement effect. From equation (29), we see that the optimal value of λ is independent of squeezing rate γ, while the squeezing effect is sensitive to the rate of Ω/ω and ϵ/ω shown in equation (30). When Ω/ω is large, the δ is nonnegligible. The difference between our method and the GVM is noticeable. In such a case, our method evidently improves the GVM. When ϵ/ω is large, the δ is small, and it implies that a large bias reduces the squeezing.

We would like to point out that the analytical method is challenged for large Ω/ω or large ϵ/ω in the sense of perturbation in equation (5). In the large Ω/ω case, we limit our discussion to the ultrastrong coupling regime ($g \lesssim \omega$). If the coupling strength becomes much larger, one oscillator approximation (single polaron picture) is not enough. In such a case, no matter how optimal the displacement and squeezing parameters are chosen, some important physics must be missed. In such a case, a novel critical regime meets. Plenty of interesting phenomena emerge [49–52].

In conclusion, in this paper we propose an approximation method to improve the GVM to study the biased QRM by introducing the squeezing transformation. Since the QRM is an oscillator-involved model, the wave packet of its ground state is naturally expected to be compressed. In the preceding literature, various transformations to the Hamiltonian are mainly limited to the displacement effect of the wave function. The comparison of several physical quantities with different parameters show that our method works well for larger coupling strength g and atom frequency Ω than the GVM. In these parameter regimes, the effect of deformation of the oscillator state can not be neglected. Thus the additional squeezing transformation brings a prominent improvement over the GVM. A natural question arises whether such approximation method considering both the displacement and the squeezing effects works well for the low-lying excited states. We hope our study is a starting point for further investigations and has potential applications in quantum thermodynamics and quantum computing, where a very accurate approximation for obtaining energy spectra is desired [53–56].

Acknowledgments

Appendix. Calculation details of equations (13) and (14)

The associated Laguerre function defined by

$$L_n^\mu(z) = \frac{(n+\mu)!}{n!\mu!} \sum_{l=0}^{\infty} \frac{(-n)(-n+1)(-n+2)\cdots(-n+l-1)}{l!(\mu+1)(\mu+2)\cdots(\mu+l)} z^l, \qquad (A.1)$$

with its reduced form, namely the Laguerre function

$$L_n(z) = L_n^0(z). \tag{A.2}$$

For the operator production, we have

$$\begin{cases} \left(a^\dagger\right)^m a^n = \left(a^\dagger\right)^{m-n} h_n(\hat{N}), & m \geqslant n \\ \left(a^\dagger\right)^m a^n = h_m(\hat{N}) a^{n-m}, & m < n \end{cases} \tag{A.3}$$

where

$$h_n(\hat{N}) = \hat{N}(\hat{N}-1)(\hat{N}-2)\cdots(\hat{N}-n+1). \tag{A.4}$$

With the above equations in hand, we can obtain

$$\begin{aligned} \cosh\nu\left(a^\dagger - a\right) &= \frac{1}{2}\left[e^\nu\left(a^\dagger - a\right) + e^{-\nu}\left(a^\dagger - a\right)\right] \\ &= \frac{1}{2}e^{-\nu^2/2}\left[e^{\nu a^\dagger}e^{-\nu a} + e^{-\nu a^\dagger}e^{\nu a}\right] \\ &= \frac{1}{2}e^{-\nu^2/2}\sum_{m,n}^{\infty}\frac{1}{m!n!}\left[\nu^m(-\nu)^n + (-\nu)^m\nu^n\right]\left(a^\dagger\right)^m a^n. \end{aligned} \tag{A.5}$$

Here, we use the formula

$$\mathrm{e}^{(A+B)} = \mathrm{e}^A \mathrm{e}^B \mathrm{e}^{-\frac{1}{2}[A,B]}. \tag{A.6}$$

For $m - n = 2k \geqslant 0$, there is

$$
\begin{aligned}
I_x^+ &= \frac{1}{2}\mathrm{e}^{-\nu^2/2} \sum_{m,n}^{\infty} \frac{1}{m!n!} \left[\nu^m(-\nu)^n + (-\nu)^m \nu^n \right] \left(a^\dagger\right)^m a^n \\
&= \frac{1}{2}\mathrm{e}^{-\nu^2/2} \sum_{k}^{\infty} \sum_{n}^{\infty} \frac{1}{(n+2k)!n!} \left[\nu^{n+2k}(-\nu)^n + (-\nu)^{(n+2k)} \nu^n \right] \left(a^\dagger\right)^{(n+2k)} a^n \\
&= \frac{1}{2}\mathrm{e}^{-\nu^2/2} \sum_{k}^{\infty} \nu^{2k} \left(a^\dagger\right)^{2k} \sum_{n}^{m} \frac{(-)^n h_n(\hat{N})}{(n+2k)!n!} \left(2\nu^{2n}\right) \\
&= \mathrm{e}^{-\nu^2/2} \sum_{k}^{\infty} \nu^{2k} \left(a^\dagger\right)^{2k} \frac{(\hat{N}+2k)!}{N!} \frac{\hat{N}!}{(\hat{N}+2k)!} \sum_{n}^{\infty} \frac{(-)^n h_n(\hat{N})}{(n+2k)!n!} \nu^{2n} \\
&= \mathrm{e}^{-\nu^2/2} \sum_{k}^{\infty} \nu^{2k} \left(a^\dagger\right) \frac{(\hat{N}+2k)!}{\hat{N}!} L_{\hat{N}}^{2k}\left(\nu^2\right).
\end{aligned}
\tag{A.7}
$$

For $m - n = -2k \leqslant 0$, there is

$$
\begin{aligned}
I_x^- &= \frac{1}{2}\mathrm{e}^{-\nu^2/2} \sum_{m,n}^{\infty} \frac{1}{m!n!} \left[\nu^m(-\nu)^n + (-\nu)^m \nu^n \right] \left(a^\dagger\right)^m a^n \\
&= \mathrm{e}^{-\nu^2/2} \sum_{k}^{\infty} \nu^{2k} \frac{(\hat{N}+2k)!}{\hat{N}!} L_N^{2k}\left(\nu^2\right) a^{2k}.
\end{aligned}
\tag{A.8}
$$

With the above all and the definition of $F_m(n)$ in equation (15), the equation (13) can be obtained after some algebra. In the similar way, equation (14) can be obtained as well.

ORCID iDs

Yimin Wang ⬤ https://orcid.org/0000-0001-8349-7515
Wen-Long You ⬤ https://orcid.org/0000-0003-1388-3861
Maoxin Liu ⬤ https://orcid.org/0000-0003-4540-4554

References

[1] Rabi I I 1936 On the process of space quantization *Phys. Rev.* **49** 324–8
[2] Rabi I I 1937 Space quantization in a gyrating magnetic field *Phys. Rev.* **51** 652–4
[3] Crespi A, Longhi S and Osellame R 2012 Photonic realization of the quantum Rabi model *Phys. Rev. Lett.* **108** 163601
[4] Wallraff A, Schuster D I, Blais A, Frunzio L, Huang R, Majer J, Kumar S, Girvin S M and Schoelkopf R J 2004 Strong coupling of a single photon to a superconducting qubit using circuit quantum electrodynamics *Nature* **431** 162–7
[5] Wallraff A, Schuster D I, Blais A, Frunzio L, Majer J, Devoret M H, Girvin S M and Schoelkopf R J 2005 Approaching unit visibility for control of a superconducting qubit with dispersive readout *Phys. Rev. Lett.* **95** 060501
[6] Ricardo P, Myung-Joong H, Jorge C and Plenio Martin B 2017 Probing the dynamics of a superradiant quantum phase transition with a single trapped ion *Phys. Rev. Lett.* **118** 073001

[7] Irish E K 2007 Generalized rotating-wave approximation for arbitrarily large coupling *Phys. Rev. Lett.* **99** 173601

[8] Yuanwei Z, Gang C, Lixian Y, Qifeng L, Liang J-Q and Suotang J 2011 Analytical ground state for the Jaynes–Cummings model with ultrastrong coupling *Phys. Rev.* A **83** 065802

[9] Mao B-B, Liu M, Wu W, Li L, Ying Z-J and Luo H-G 2018 An analytical variational method for the biased quantum Rabi model in the ultra-strong coupling regime *Chin. Phys.* B **27** 054219

[10] Lixian Y, Shiqun Z, Qifeng L, Gang C and Suotang J 2012 Analytical solutions for the Rabi model *Phys. Rev.* A **86** 015803

[11] Yu-Yu Z, Qing-Hu C and Yang Z 2013 Generalized rotating-wave approximation to biased qubit-oscillator systems *Phys. Rev.* A **87** 033827

[12] Maoxin L, Zu-Jian Y, Jun-Hong A and Hong-Gang L 2015 Mean photon number dependent variational method to the Rabi model *New J. Phys.* **17** 043001

[13] Yu-Yu Z and Qing-Hu C 2015 Generalized rotating-wave approximation for the two-qubit quantum Rabi model *Phys. Rev.* A **91** 013814

[14] Lijun M, Yanxia L and Yunbo Z 2016 Entanglement dynamics of the ultrastrong-coupling three-qubit Dicke model *Phys. Rev.* A **93** 052305

[15] Yu-Yu Z 2016 Generalized squeezing rotating-wave approximation to the isotropic and anisotropic Rabi model in the ultrastrong-coupling regime *Phys. Rev.* A **94** 063824

[16] Yu-Yu Z, Xiang-You C, Shu H and Qing-Hu C 2016 Analytical solutions and genuine multipartite entanglement of the three-qubit dicke model *Phys. Rev.* A **94** 012317

[17] Ni L, Jiangdan L and Liang J-Q 2013 Nonequilibrium quantum phase transition of Bose–Einstein condensates in an optical cavity *Phys. Rev.* A **87** 053623

[18] Wang Z H, Yong L, Zhou D L, Sun C P and Peng Z 2012 Single-photon scattering on a strongly dressed atom *Phys. Rev.* A **86** 023824

[19] Gan C J and Zheng H 2010 Dynamics of a two-level system coupled to a quantum oscillator: transformed rotating-wave approximation *Eur. Phys. J.* D **59** 473–8

[20] Yiying Y, Zhiguo L and Hang Z 2015 Bloch–Siegert shift of the Rabi model *Phys. Rev.* A **91** 053834

[21] Bin-Bin M, Liangsheng L, Yimin W, Wen-Long Y, Wei W, Maoxin L and Hong-Gang L 2019 Variational generalized rotating-wave approximation in the two-qubit quantum Rabi model *Phys. Rev.* A **99** 033834

[22] Braak D 2011 IntegRability of the Rabi model *Phys. Rev. Lett.* **107** 100401

[23] Honghua Z, Qiongtao X, Batchelor M T and Chaohong L 2013 Analytical eigenstates for the quantum Rabi model *J. Phys. A: Math. Theor.* **46** 415302

[24] Qing-Hu C, Chen W, Shu H, Tao L and Ke-Lin W 2012 Exact solvability of the quantum Rabi model using bogoliubov operators *Phys. Rev.* A **86** 023822

[25] Jaynes E T and Cummings F W 1963 Comparison of quantum and semiclassical radiation theories with application to the beam maser *Proc. IEEE* **51** 89–109

[26] Forn-Díaz P, García-Ripoll J J, Peropadre B, Orgiazzi J-L, Yurtalan M A, Belyansky R, Wilson C M and Lupascu A 2017 Ultrastrong coupling of a single artificial atom to an electromagnetic continuum in the nonperturbative regime *Nat. Phys.* **13** 39–43

[27] Fumiki Y, Tomoko F, Sahel A, Kosuke K, Shiro S and Kouichi S 2017 Superconducting qubit-oscillator circuit beyond the ultrastrong-coupling regime *Nat. Phys.* **13** 44–7

[28] Zhen C *et al* 2017 Single-photon-driven high-order sideband transitions in an ultrastrongly coupled circuit-quantum-electrodynamics system *Phys. Rev.* A **96** 012325

[29] Niemczyk T *et al* 2010 Circuit quantum electrodynamics in the ultrastrong-coupling regime *Nat. Phys.* **6** 772

[30] Forn-Díaz P, Lisenfeld J, Marcos D, García-Ripoll J J, Solano E, Harmans C J and Mooij J E 2010 Observation of the bloch-siegert shift in a qubit-oscillator system in the ultrastrong coupling regime *Phys. Rev. Lett.* **105** 237001

[31] Goda K, Miyakawa O, Mikhailov E E, Saraf S, Adhikari R, Mckenzie K, Ward R, Vass S, Weinstein A J and Mavalvala N 2008 A quantum-enhanced prototype gravitational-wave detector *Nat. Phys.* **4** 472–6

[32] Wineland D J, Bollinger J J, Itano W M and Heinzen D J 1994 Squeezed atomic states and projection noise in spectroscopy *Phys. Rev.* A **50** 67–88

[33] Sørensen J L, Hald J and Polzik E S 1998 Quantum noise of an atomic spin polarization measurement *Phys. Rev. Lett.* **80** 3487–90

[34] Jun Y, Kimble H J and Hidetoshi K 2008 Quantum state engineering and precision metrology using state-insensitive light traps *Science* **320** 1734–8

J. Phys. A: Math. Theor. **53** (2020) 095302

W Xie *et al*

[35] Furusawa A, Sørensen J L, Braunstein S L, Fuchs C A, Kimble H J and Polzik E S 1998 Unconditional quantum teleportation *Science* **282** 706–9

[36] Kheruntsyan K V, Olsen M K and Drummond P D 2005 Einstein–Podolsky–Rosen correlations via dissociation of a molecular Bose–Einstein condensate *Phys. Rev. Lett.* **95** 150405

[37] Wüster S, Dabrowska-Wüster B J, Scott S M, Close J D and Savage C M 2008 Quantum-field dynamics of expanding and contracting Bose–Einstein condensates *Phys. Rev.* A **77** 023619

[38] Haine Simon A and Johnsson Mattias T 2009 Dynamic scheme for generating number squeezing in Bose–Einstein condensates through nonlinear interactions *Phys. Rev.* A **80** 023611

[39] Döring D, McDonald G, Debs J E, Figl C, Altin P A, Bachor H-A, Robins N P and Close J D 2010 Quantum-projection-noise-limited interferometry with coherent atoms in a ramsey-type setup *Phys. Rev.* A **81** 043633

[40] Johnsson M T and Haine S A 2007 Generating quadrature squeezing in an atom laser through self-interaction *Phys. Rev. Lett.* **99** 010401

[41] Yu-Yu Z and Xiang-You C 2017 Analytical solutions by squeezing to the anisotropic Rabi model in the nonperturbative deep-strong-coupling regime *Phys. Rev.* A **96** 063821

[42] Honghua Z, Qiongtao X, Xiwen G, Batchelor M T, Kelin G and Chaohong L 2014 Analytical energy spectrum for hybrid mechanical systems *J. Phys. A: Math. Theor.* **47** 045301

[43] Qiongtao X, Honghua Z, Batchelor M T and Chaohong L 2017 The quantum Rabi model: solution and dynamics *J. Phys. A: Math. Theor.* **50** 113001

[44] Zi-Min L and Batchelor M T 2015 Algebraic equations for the exceptional eigenspectrum of the generalized Rabi model *J. Phys. A: Math. Theor.* **48** 454005

[45] Zi-Min L and Batchelor M T 2016 Addendum to algebraic equations for the exceptional eigenspectrum of the generalized Rabi model *J. Phys. A: Math. Theor.* **49** 369401

[46] Irish E K, Gea-Banacloche J, Martin I and Schwab K C 2005 Dynamics of a two-level system strongly coupled to a high-frequency quantum oscillator *Phys. Rev.* B **72** 195410

[47] Zu-Jian Y, Maoxin L, Hong-Gang L, Hai-Qing L and You J Q 2015 Ground-state phase diagram of the quantum Rabi model *Phys. Rev.* A **92** 053823

[48] Lei C, Xi-Mei S, Maoxin L, Zu-Jian Y and Hong-Gang L 2017 Frequency-renormalized multipolaron expansion for the quantum Rabi model *Phys. Rev.* A **95** 063803

[49] Myung-Joong H, Ricardo P and Plenio M B 2015 Quantum phase transition and universal dynamics in the Rabi model *Phys. Rev. Lett.* **115** 180404

[50] Myung-Joong H and Plenio M B 2016 Quantum phase transition in the finite Jaynes–Cummings lattice systems *Phys. Rev. Lett.* **117** 123602

[51] Yimin W, Wen-Long Y, Maoxin L, Yu Li D and You J Q 2018 Controllable anisotropic quantum Rabi model beyond the ultrastrong coupling regime with circuit qed systems *New J. Phys.* **20** 053061

[52] Maoxin L, Stefano C, Zu-Jian Y, Xiaosong C, Hong-Gang L and Hai-Qing L 2017 Universal scaling and critical exponents of the anisotropic quantum Rabi model *Phys. Rev. Lett.* **119** 220601

[53] Barrios G A, Albarrán-Arriagada F, Cárdenas-López F A, Romero G and Retamal J C 2017 Role of quantum correlations in light-matter quantum heat engines *Phys. Rev.* A **96** 052119

[54] Albarrán-Arriagada F, Lamata L, Solano E, Romero G and Retamal J C 2018 Spin-1 models in the ultrastrong-coupling regime of circuit QED *Phys. Rev.* A **97** 022306

[55] Ferdi A, Hardal A U C and Müstecaplıoğlu Ö E 2015 Rabi model as a quantum coherent heat engine: from quantum biology to superconducting circuits *Phys. Rev.* A **91** 023816

[56] Yimin W, Jiang Z, Chunfeng W, You J Q and Romero G 2016 Holonomic quantum computation in the ultrastrong-coupling regime of circuit QED *Phys. Rev.* A **94** 012328